

Lorentz transformation as a problem of vector field flow

Shao-Hsuan Chiu^{1*} and T. K. Kuo^{2†}

¹*Department of Physics, Frostburg State University, Frostburg, MD 21532, USA*

²*Department of Physics, Purdue University, West Lafayette, IN 47907, USA*

Abstract

We study the Lorentz transformation as a vector field flow problem using the 2×2 spinor algebra. The exact, finite Thomas rotation angle is determined and interpreted intuitively. We also establish an invariant and examine the general features of the Lorentz transformation using the phase portraits of the parameters.

*Email address: schiu@frostburg.edu

†Email address: tkkuo@physics.purdue.edu

I. INTRODUCTION

One of the basic questions in the Lorentz transformation is velocity addition. Although algebraic formulas exist [1], the velocity transformations are quite complicated owing to their non-commutative nature. The conceptual complexity arises partially from the counterintuitive consequences of the Thomas rotation. Furthermore, the determination of the transformation parameters is in general quite involved. It would therefore be useful to gain a general picture of the behavior of the transformation from a simple, intuitive approach. Interestingly, it has recently been shown [2] that the two-flavor neutrino mass matrix in the seesaw model [3] exhibits a Lorentz group-like structure, from which the constraint on the mixing angle and the hierarchical structure of the neutrino masses can be established. On the other hand, the RGE (Renormalization Group Equation) running of the neutrino mass and mixing angle between high and low energy scales can be illustrated as the flow of vector field [4]. The Lorentz transformation as a vector field flow problem has not been investigated in detail even though there seems an inherent connection between them. We shall show that the vector field flows and the fixed points provide a clear view of the Lorentz velocity transformations. Starting from the simple commutation relations of the 2×2 spinor algebra, we first obtain the Lorentz velocity transformation and the exact, finite Thomas rotation angle associated with the transformation. We then derive the differential equations for the parameters and illustrate their properties in the phase portraits. As an example, the collimation effect of the relativistic decay is interpreted as a vector field flow problem. In addition, an invariant governing the evolution of velocity and direction in the Lorentz velocity addition is established.

The order of successive Lorentz transformations plays a crucial role when two inertial reference frames are related. This property is indicated by the commutation relations [5]:

$$\begin{aligned} [J_i, J_j] &= i\epsilon_{ijk}J_k, \\ [J_i, K_j] &= i\epsilon_{ijk}K_k, \\ [K_i, K_j] &= -i\epsilon_{ijk}J_k, \end{aligned} \tag{1}$$

where $J_{i,j,k}$ and $K_{i,j,k}$ are the infinitesimal generators of rotations and pure Lorentz boosts, respectively. The Thomas precession is known to originate from this non-commutability of the generators: A new reference frame reached by two successive Lorentz boosts cannot be reached by a third, pure boost from the original frame without a Thomas rotation. In the literature, the infinitesimal Thomas rotation angle is usually calculated from a continuous application of infinitesimal Lorentz transformations consisting of rotations and boosts [1], while the finite Thomas rotation angle can be determined by a variety of approaches [6–8]. In this article we employ the simple properties of Pauli matrices instead, for the determination of finite Thomas rotation angle as well as other parameters in the Lorentz velocity transformations.

II. LORENTZ VELOCITY TRANSFORMATION

In the two-component spinor algebra, Pauli matrices satisfy the commutator:

$$[\sigma_i, \sigma_j] = 2i\epsilon_{ijk}\sigma_k. \tag{2}$$

It is clear that $J_i = \sigma_i/2$ (rotations) and $K_i = i\sigma_i/2$ (boosts) are two-dimensional representations of the Lorentz group: A finite rotation about an arbitrary axis \hat{n} through an angle Θ is written as $\mathbf{R} = \exp(\frac{i\Theta\vec{\sigma}\cdot\hat{n}}{2})$, while $\mathbf{B} = \exp(\frac{-\kappa\vec{\sigma}\cdot\hat{n}}{2})$ represents a pure boost along an arbitrary direction \hat{n} , with κ the rapidity parameter. Without loss of generality, we consider the addition of two pure boosts by choosing one boost of rapidity parameter η along the direction $\hat{n}_{\theta_0} = (\sin \theta_0 \hat{x} + \cos \theta_0 \hat{z})$:

$$\beta_1 = \tanh \eta (\sin \theta_0 \hat{x} + \cos \theta_0 \hat{z}), \quad (3)$$

and the other of rapidity ξ along \hat{z} :

$$\beta_2 = \tanh \xi \hat{z}, \quad (4)$$

as shown in Fig.1. The combination of the two pure boosts

$$L = e^{-\frac{\xi}{2}\vec{\sigma}\cdot\hat{z}} e^{-\frac{\eta}{2}\vec{\sigma}\cdot\hat{n}_{\theta_0}} = e^{-\frac{\xi}{2}\sigma_3} e^{-\frac{\eta}{2}(\sigma_3 \cos \theta_0 + \sigma_1 \sin \theta_0)} \quad (5)$$

is equivalent to a third boost plus a rotation about an axis parallel to \hat{y} :

$$\begin{aligned} L &= e^{-\frac{\lambda}{2}(\sigma_3 \cos \theta + \sigma_1 \sin \theta)} e^{i\frac{\tau}{2}\sigma_2} \\ &= e^{-i\frac{\theta}{2}\sigma_2} e^{-\frac{\lambda}{2}\sigma_3} e^{i\frac{\theta+\tau}{2}\sigma_2}, \end{aligned} \quad (6)$$

where τ the is the Thomas rotation angle and λ represents the third rapidity in the direction $\hat{n}_\theta = (\sin \theta \hat{x} + \cos \theta \hat{z})$, with $0 \leq \theta \leq \pi$. Given two boosts of parameters ξ and η , which are separated by an angle θ_0 , the new parameters λ , θ , and in particular, the angle τ , can be derived exactly. We first note that the simple product LL^T leads to λ and θ [2]. From eq.(5), LL^T can be written as:

$$\begin{aligned} LL^T &= e^{-\frac{\xi}{2}\sigma_3} e^{-\eta(\sigma_3 \cos \theta_0 + \sigma_1 \sin \theta_0)} e^{-\frac{\xi}{2}\sigma_3} \\ &= \cosh \xi \cosh \eta + \cos \theta_0 \sinh \xi \sinh \eta - \\ &\quad [\sinh \xi \cosh \eta + \cos \theta_0 \cosh \xi \sinh \eta] \sigma_3 \\ &\quad - [\sin \theta_0 \sinh \eta] \sigma_1, \end{aligned} \quad (7)$$

while from eq.(6):

$$\begin{aligned} LL^T &= e^{-\lambda(\sigma_3 \cos \theta + \sigma_1 \sin \theta)} = e^{-i\frac{\theta}{2}\sigma_2} e^{-\lambda\sigma_3} e^{i\frac{\theta}{2}\sigma_2} \\ &= \cosh \lambda - (\sigma_3 \cos \theta + \sigma_1 \sin \theta) \sinh \lambda. \end{aligned} \quad (8)$$

Note that the Thomas precession angle τ is canceled out in LL^T . By comparing eqs.(7) and (8), we immediately get

$$\tan \theta = \frac{\sin \theta_0 \sinh \eta}{\sinh \xi \cosh \eta + \cos \theta_0 \cosh \xi \sinh \eta}, \quad (9)$$

$$\cosh \lambda = \cosh \xi \cosh \eta + \cos \theta_0 \sinh \xi \sinh \eta. \quad (10)$$

The above two equations are equivalent to eq.(11.32) in Jackson [1].

III. THE THOMAS ROTATION ANGLE

To derive τ , we now consider $L^T L$. From eq.(5),

$$L^T L = e^{-\frac{\eta}{2}(\sigma_3 \cos \theta_0 + \sigma_1 \sin \theta_0)} e^{-\xi \sigma_3} e^{-\frac{\eta}{2}(\sigma_3 \cos \theta_0 + \sigma_3 \sin \theta_0)}, \quad (11)$$

while eq.(6) gives

$$L^T L = e^{-i\frac{\theta+\tau}{2}\sigma_2} e^{-\lambda \sigma_3} e^{i\frac{\theta+\tau}{2}\sigma_2}. \quad (12)$$

Eq.(11) can further be simplified by using the identity

$$e^{-i\frac{\theta_0}{2}\sigma_2} e^{-\frac{\eta}{2}\sigma_3} e^{i\frac{\theta_0}{2}\sigma_2} = e^{-\frac{\eta}{2}(\sigma_3 \cos \theta_0 + \sigma_1 \sin \theta_0)}, \quad (13)$$

which leads to

$$L^T L = e^{-i\frac{\theta_0}{2}\sigma_2} (e^{-\frac{\eta}{2}\sigma_3} e^{-\xi \sigma_{(-\theta_0)}} e^{-\frac{\eta}{2}\sigma_3}) e^{i\frac{\theta_0}{2}\sigma_2}, \quad (14)$$

where $\sigma_{(-\theta_0)} \equiv \sigma_3 \cos(-\theta_0) + \sigma_1 \sin(-\theta_0)$. We then obtain a simple relation from eqs.(12) and (14):

$$e^{-i\frac{\theta+\tau-\theta_0}{2}\sigma_2} e^{-\lambda \sigma_3} e^{i\frac{\theta+\tau-\theta_0}{2}\sigma_2} = e^{-\frac{\eta}{2}\sigma_3} e^{-\xi \sigma_{(-\theta_0)}} e^{-\frac{\eta}{2}\sigma_3}. \quad (15)$$

With the substitutions $\eta \rightarrow \xi$, $\xi \rightarrow \eta$, and $-\theta_0 \rightarrow \theta_0$, the right-hand side of eq.(15) is just LL^T in eq.(7). This allows us to read off $\tan(\theta + \tau - \theta_0)$ directly from eq.(9):

$$\tan(\theta + \tau - \theta_0) \equiv \tan \phi = \frac{-\sin \theta_0 \sinh \xi}{\cosh \xi \sinh \eta + \cos \theta_0 \sinh \xi \cosh \eta}. \quad (16)$$

Here, ϕ specifies the direction of the resultant third boost when β_1 and β_2 are applied in a reverse order. The finite Thomas rotation angle is given by $\tau = \phi + \theta_0 - \theta$, and

$$\tan \tau = \frac{\tan \phi + \tan(\theta_0 - \theta)}{1 - \tan \phi \tan(\theta_0 - \theta)}. \quad (17)$$

Note that τ is expressed in terms of η , ξ , and θ_0 .

The results in eqs.(9), (10), and (17) are exact, and valid for the finite Lorentz transformations without resorting to any successive application of infinitesimal transformations. To check whether eq.(17) reduces to the result in Section 11.8 of Ref. [1] under infinitesimal Lorentz transformation, we consider a finite boost $\beta_1 = \tanh \eta$, followed by an infinitesimal boost $\beta_2 = \tanh(\Delta \xi) \cong \Delta \xi$. Eqs.(9) and (16) yield

$$\tan \theta \cong \tan \theta_0 \left(1 - \frac{\coth \eta}{\cos \theta_0} \Delta \xi\right) \quad (18)$$

and

$$\tan \phi \cong \frac{-\sin \theta_0}{\sinh \eta} \Delta \xi, \quad (19)$$

respectively. The infinitesimal Thomas rotation angle then becomes

$$\Delta\tau \cong \frac{\sin\theta_0}{\sinh\eta}(\cosh\eta - 1)\Delta\xi. \quad (20)$$

In Ref. [1], the infinitesimal Thomas rotation angle is shown to be

$$\Delta\Omega = \frac{\gamma^2}{\gamma + 1}\boldsymbol{\beta} \times \delta\boldsymbol{\beta} \quad (21)$$

Note that our notations and that of Ref. [1] are slightly different. Our $\boldsymbol{\beta}_1$ and $\boldsymbol{\beta}_2$ correspond to $\boldsymbol{\beta}$ and $\gamma^2\delta\boldsymbol{\beta}_{\parallel} + \gamma\delta\boldsymbol{\beta}_{\perp}$ in Ref. [1], respectively. Thus,

$$\begin{aligned} \Delta\Omega &= \frac{\gamma^2}{\gamma + 1}\boldsymbol{\beta} \times \delta\boldsymbol{\beta} \\ &= \frac{\gamma^2}{\gamma + 1}\boldsymbol{\beta} \times \delta\boldsymbol{\beta}_{\perp}, \end{aligned} \quad (22)$$

which is equivalent to $(\gamma^2/\gamma + 1)\boldsymbol{\beta}_1 \times (\boldsymbol{\beta}_2/\gamma)$ in our notation. Therefore,

$$\Delta\Omega = \frac{\sin\theta_0}{\sinh\eta}(\cosh\eta - 1)\Delta\xi, \quad (23)$$

and it agrees with eq.(20). We also note that eq.(17) agrees with eq.(37) of Ref. [8] up to an overall sign, which is due merely to the different sense of rotation.

An alternative physical interpretation of the Thomas rotation angle becomes clear from our formulation as we examine two boosts combined in reverse orders. From eq.(5) and eq.(6),

$$e^{-\frac{\xi}{2}\sigma_3}e^{-\frac{\eta}{2}\sigma_{\theta_0}} = e^{-\frac{\lambda}{2}\sigma_{\theta}}e^{i\frac{\tau}{2}\sigma_2}, \quad (24)$$

where $\sigma_{\theta_0} \equiv \sigma_3 \cos\theta_0 + \sigma_1 \sin\theta_0$, and $\sigma_{\theta} \equiv \sigma_3 \cos\theta + \sigma_1 \sin\theta$. It follows that

$$e^{-\frac{\xi}{2}\sigma_3}e^{-\frac{\eta}{2}\sigma_{\theta_0}}e^{-i\frac{\tau}{2}\sigma_2} = e^{-\frac{\lambda}{2}\sigma_{\theta}}. \quad (25)$$

Note that σ_1 and σ_3 are symmetric while σ_2 is antisymmetric:

$$(e^{-\frac{\lambda}{2}\sigma_{\theta}})^T = e^{-\frac{\lambda}{2}\sigma_{\theta}} = e^{-\frac{\xi}{2}\sigma_3}e^{-\frac{\eta}{2}\sigma_{\theta_0}}e^{-i\frac{\tau}{2}\sigma_2}. \quad (26)$$

After taking the transpose, the left-hand side of eq.(25) becomes $e^{i\frac{\tau}{2}\sigma_2}e^{-\frac{\eta}{2}\sigma_{\theta_0}}e^{-\frac{\xi}{2}\sigma_3}$. This leads us to the relation:

$$e^{i\frac{\tau}{2}\sigma_2}(e^{-\frac{\eta}{2}\sigma_{\theta_0}}e^{-\frac{\xi}{2}\sigma_3})e^{i\frac{\tau}{2}\sigma_2} = e^{-\frac{\xi}{2}\sigma_3}e^{-\frac{\eta}{2}\sigma_{\theta_0}}. \quad (27)$$

Eq.(27) implies that the combination of two boosts, $\exp(-\frac{\xi}{2}\sigma_3)\exp(-\frac{\eta}{2}\sigma_{\theta_0})$, is related to the reverse, $\exp(-\frac{\eta}{2}\sigma_{\theta_0})\exp(-\frac{\xi}{2}\sigma_3)$, by two identical rotations, $e^{i\frac{\tau}{2}\sigma_2}$. In other words, operating a rotation on a reference frame before and after two successive boosts would bring this frame to the same reference frame that is reached by the same two boosts operated in reverse order. The angle associates with this particular rotation is the Thomas rotation angle.

IV. LORENTZ VELOCITY TRANSFORMATIONS AS VECTOR FIELD FLOWS

We now turn to the vector field flow problem. Some qualitative observations are in order here:

(I). In the limit where the second boost vanishes ($\xi = 0$), one would expect the Thomas rotation angle to vanish ($\tau = 0$) as well. In addition, $\theta = \theta_0$ and $\lambda = \eta$ when $\xi = 0$.

(II). As the second rapidity ξ increases by $d\xi$ from zero, θ decreases by $d\theta$ from θ_0 , λ increases by $d\lambda$ from η for $0 < \theta < \pi/2$ (or decreases by $d\lambda$ from η for $\pi/2 < \theta < \pi$), and τ increases by $d\tau$ from zero.

Following these lines three differential equations for θ , β ($\beta \equiv \tanh \lambda$), and τ can be derived from eqs.(9), (10), and (17):

$$\frac{d\theta}{d\xi} = \frac{-\sin \theta}{\beta}, \quad (28)$$

$$\frac{d\beta}{d\xi} = \cos \theta (1 - \beta^2), \quad (29)$$

$$\frac{d\tau}{d\xi} = \frac{\sin \theta}{\beta} (1 - \sqrt{1 - \beta^2}). \quad (30)$$

There are four fixed points for the evolution equations, eqs.(28) and (29): $(\beta, \theta) = (1, 0)$, $(-1, \pi)$, $(1, \pi)$, and $(-1, 0)$. The stability [10] of the fixed points as ξ increases are determined by the eigenvalues of the Jacobian. Of the four fixed points, $(1, 0)$ and $(-1, \pi)$ are stable (attractive) and the evolution of θ and β is always toward one of the two points. On the other hand, the evolution is always directed away from the unstable (repulsive) fixed points, $(1, \pi)$ and $(-1, 0)$. Note that the two attractive fixed points are physically identical, so are the two repulsive fixed points. This is because β of opposite signs simply represent boosts in opposite directions. The $\theta - \beta$ phase portrait is shown in Fig.2, where the direction fields are plotted for increasing ξ and the arrows are tangent to the trajectories. The phase portrait illustrates the following features:

(I). As ξ evolves, all the trajectories evolve from their respective initial conditions toward the stable fixed points $(\beta, \theta) = (1, 0)$ or $(\beta, \theta) = (-1, \pi)$, depending on the signs of the boosts. This simply means that the resultant third boost β tends to evolve from its initial value toward $|\beta| = 1$, and its direction evolves toward that of the second boost β_2 . The evolution of direction also can be understood from eq.(28): $\frac{d\theta}{d\xi} \geq 0$ for a negative β and $\frac{d\theta}{d\xi} \leq 0$ for a positive β .

(II). The long arrows near the region of small $|\beta|$ and large $\sin \theta$ ($\theta \approx \pi/2$) indicate a rapid variation of β 's direction. This is also implied by eq.(28).

(III). For $|\beta| = 1$, the slope of the trajectory becomes infinity and the transformation does not exist. Physically, this can be interpreted as no transformation from the rest frame of a photon to a laboratory frame.

The fixed point of Lorentz velocity addition can be understood in the well known collimation effect of relativistic decays, e.g., $\pi^0 \rightarrow \gamma\gamma$. For fast moving π^0 , most photons are emitted forward. This corresponds to $\theta \rightarrow 0$ and $\beta \rightarrow 1$ as $\beta_2 \rightarrow 1$, which is a fixed point of the vector field flow.

We next examine the relation between the two angles, θ and τ . From eq.(30) we see that at small $|\beta|$, the Thomas rotation angle τ does not vary significantly with ξ : $\frac{d\tau}{d\xi} \approx 0$, while θ varies rapidly according to eq.(28). On the other hand, $\frac{d\theta}{d\xi}$ slows down and $\frac{d\tau}{d\xi}$ speeds up as $|\beta|$ increases. This feature is also clearly indicated by the solution of a differential equation, which is obtained from dividing eq.(30) by eq.(28):

$$\frac{d\tau}{d\theta} = -(1 - \sqrt{1 - \beta^2}). \quad (31)$$

The solution is given by

$$\tau - \tau_0 = \frac{1 - \gamma}{\gamma}(\theta - \theta_0), \quad (32)$$

where $\gamma \equiv 1/\sqrt{1 - \beta^2}$. For a given $|\beta|$, eq.(28) implies that the rate of change of θ is maximum at $\theta = \pi/2$, where the two boosts are perpendicular. In addition, eqs.(16) and (17) imply that if $\beta_1 \approx 1$ and $\beta_2 \approx 1$, then $\tan \phi \cong 0$ and $\tau \cong \theta_0$. Therefore, when the two successive boosts are each close to light speed, the Thomas rotation angle associated with the transformation approaches the angle between the two boosts. Furthermore, $\tau = 0$ if the two successive boosts are co-linear.

The evolution of β , θ , and τ can be visualized from a 3-D phase portrait. In Fig.3 the initial conditions corresponding to $\beta_2 = 0$ and arbitrary (β_1, θ_0) lie in the plane specified by $\tau = 0$. As β_2 increases, θ and β evolve along one of the trajectories in Fig.2 while changing the corresponding τ value at varying rates. This rate of change of τ is determined by the local values of β and θ as implied by eq.(30). If the initial β_2 is chosen to be nonzero, the initial conditions lie in a plane specified by a nonzero τ .

It is worthwhile to point out an invariant of the transformation. We may divide eq.(28) by eq.(29) to obtain

$$\frac{d\theta}{d\beta} = \frac{-\tan \theta}{\beta(1 - \beta^2)}. \quad (33)$$

The solution to this differential equation describes the trajectories in Fig.2:

$$\sin \theta \sinh \lambda = \sin \theta_0 \sinh \lambda_0. \quad (34)$$

This invariant regulates the evolution of direction and magnitude of the resultant boost. Note that the Thomas rotation angle τ does not take part in this invariant. We also note that in the analysis of neutrino parameters [2], θ and $e^{2\lambda}$ represent the mixing angle and the physical neutrino mass ratio, respectively.

Simple properties of the spinor algebra provide a general and effective solution to the problems of finite Lorentz velocity transformations. In particular, the exact solution of the finite Thomas rotation angle can be determined and the result leads directly to an intuitive physical interpretation of the Thomas rotation angle. Following this line, we treat the Lorentz velocity transformation as a vector field flow problem. The general features of the Lorentz transformation and the evolution of the parameters are clearly visualized using the phase portraits of the parameters. The invariant, eq.(34), carries the same form as the general, complex RGE invariant [4]. However, unlike the running of RGEs for the general

neutrino mass matrix, in which the relative phase of the mass eigenvalues is nonzero and the evolution depends sensitively on the choice of initial conditions, the Lorentz velocity transformation corresponds to a vanishing relative phase and the evolution of parameters is not as sensitive to the initial conditions, i.e., physically there is only one attractive fixed point and one repulsive fixed point.

ACKNOWLEDGMENTS

We thank H. Urbantke for pointing out Refs. [6] and [7]. T. K. K. is supported in part by DOE grant No. DE-FG02-91ER40681.

REFERENCES

- [1] J. D. Jackson, *Classical Electrodynamics* (2nd Edition), John Wiley & Sons (1975), Chapter 11.
- [2] T. K. Kuo, G.-H. Wu, and S.-H. Chiu , Phys. Rev. **D62**, 051301 (2000), hep-ph/0003066; T. K. Kuo, S.-H. Chiu, and G.-H. Wu, Eur. Phys. J. **C21**, 281-289 (2001), hep-ph/0011058.
- [3] M. Gell-Mann, P. Ramond, and R. Slansky, in *Supergravity*, eds. P. van Nieuwenhuizen and D. Freeman, North Holland, Amsterdam (1979); T. Yanagida, in *Proceedings of the Workshop on the Unified Theory and Baryon Number in the Universe*. eds. O. Sawada and A. Sugamoto, KEK (1979).
- [4] See, e.g., T. K. Kuo, J. Pantaleone, and G.-H. Wu, Phys. Lett. **B528**, 101 (2001), hep-ph/0104131, and the references therein.
- [5] See, e.g., L. H. Ryder, *Quantum Field Theory*, Cambridge University Press (1985).
- [6] A. J. MacFarlane, J. Math. Phys. **3**, 1116-1129 (1962).
- [7] H. Urbantke, Am. J. Phys. **58**, 747 (1990).
- [8] A. A. Ungar, Am. J. Phys. **59**, 824 (1991).
- [9] C. Misner, K. Thorne, and J. Wheeler, *Gravitation*, W. H. Freeman and Company (1975), Chapter 41.
- [10] S. Strogatz, *Nonlinear Dynamics and Chaos* (1994), Perseus Publishing, Cambridge, Massachusetts.

FIGURES

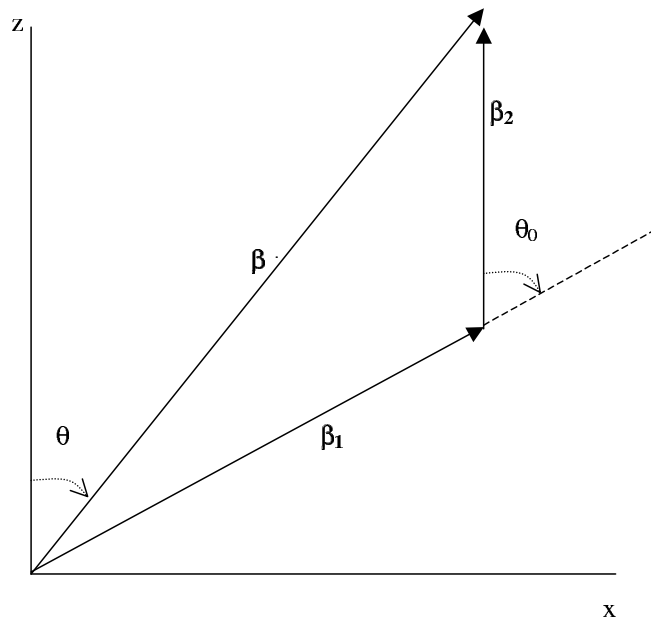


FIG. 1. The combination of two boosts, β_1 and β_2 , is equivalent to a third boost β plus a rotation about \hat{y} .

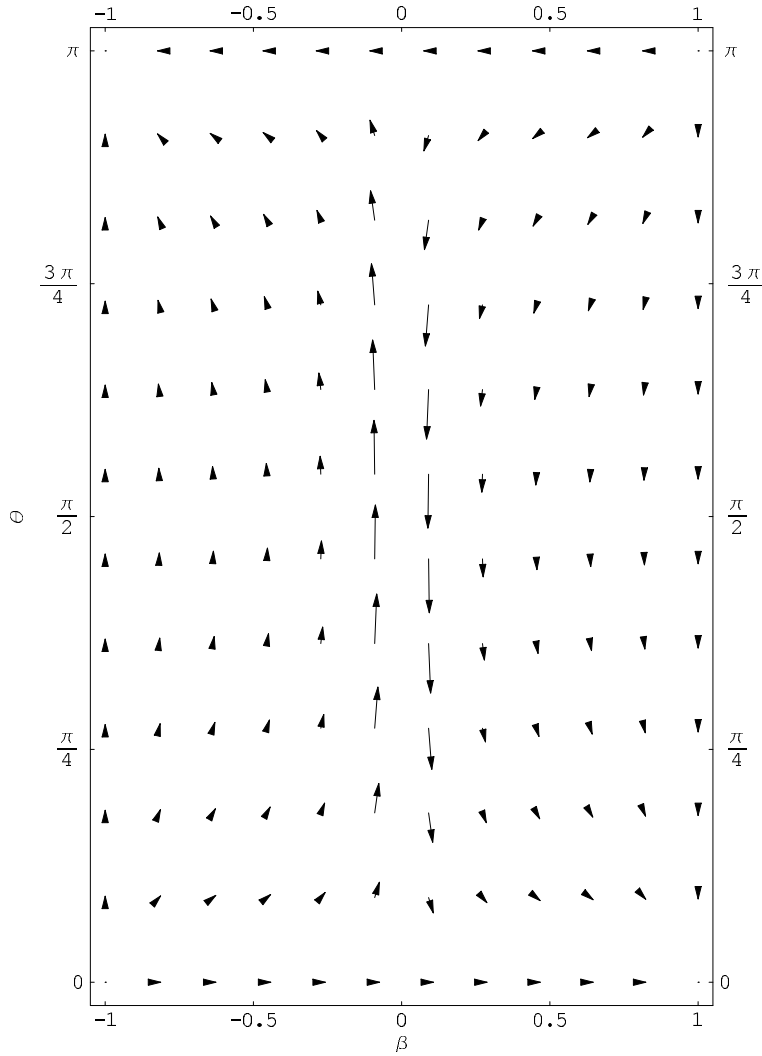


FIG. 2. The $\theta - \beta$ phase portrait. All trajectories evolve toward either $(\beta, \theta) = (1, 0)$ or $(\beta, \theta) = (1, \pi)$. Note that negative β represents a boost in the direction opposite to that of a positive β . The trajectories are described by eq.(33).

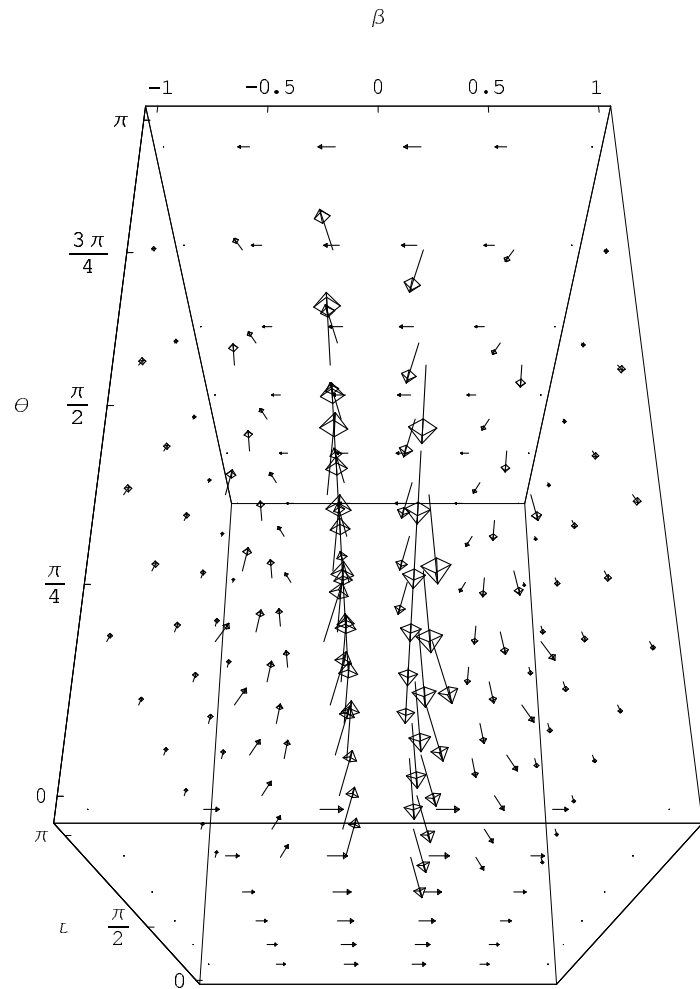


FIG. 3. The evolution of β , θ , and τ . Note that as $\beta \rightarrow 1$, (θ, τ) approaches $(0, \pi)$ for $\beta > 0$ and that (θ, τ) approaches $(\pi, -\pi)$ for $\beta < 0$. Fig.2 corresponds to a “slice” of this figure with a specific τ value. The rate of change of τ depends on the local values of β and θ .